Drift mobility of long-living excitons in coupled GaAs quantum wells

A. Gärtner, A. W. Holleitner,[a)] and J. P. Kotthaus
Department für Physik, Ludwig-Maximilians-Universität, Geschwister-Scholl-Platz 1, D-80539 München, Germany and Center for NanoScience, Ludwig-Maximilians-Universität, Geschwister-Scholl-Platz 1, D-80539 München, Germany

D. Schuh
Institut für Angewandte und Experimentelle Physik, Universität Regensburg, Universitätsstraße 31, D-93040 Regensburg, Germany

The authors report on high-mobility transport of indirect excitons in coupled GaAs quantum wells. A voltage-tunable in-plane potential gradient is defined for excitons by exploiting the quantum confined Stark effect in combination with a lithographically designed resistive top gate. Excitonic photoluminescence resolved in space, energy, and time provides insight into the in-plane drift dynamics. Across several hundreds of microns an excitonic mobility of 10^5 cm^2/eV s is observed for temperatures below 10 K. With increasing temperature the excitonic mobility decreases due to exciton-phonon scattering. © *2006 American Institute of Physics*. [DOI: 10.1063/1.2267263]

The pioneering work of Keldysh and Kozlov in 1968 has triggered many experiments aiming to observe the bosonic nature of excitons in solid-state systems.[1] For detecting the Bose-Einstein condensation of excitons, it is a prerequisite to define controllable confinement potentials for excitons. So far trapping of excitons has been demonstrated in strained systems,[2–4] magnetic traps,[5] "natural traps" defined by interface roughness fluctuations,[6] and electrostatic traps.[7–10] Only the latter enable *in situ* control of the trapping potential. In addition, electrostatic traps can be extended towards optoelectronic solid-state devices due to their potential scalability and compatibility with existing semiconductor technology.

Here we investigate the drift dynamics of long-living excitons in coupled quantum wells (QWs) in a voltage-tunable semiconductor device. In prior experiments on coupled GaAs/AlAs QWs a static, spatially resolved photoluminescence (PL) spectroscopy has been used to detect excitonic drift.[11] We extend this approach towards time-of-flight (TOF) experiments in coupled GaAs QWs by detecting the excitonic PL as a function of space, energy, and time. The technique relies on the quantum confined Stark effect (QCSE), and it allows distinguishing the dynamics of excitons from electron-hole effects.[9] In a field effect structure such as shown in Fig. 1(a), electrons and holes of photogenerated excitons may rearrange in a way that they are spatially separated by the tunnel barrier between the GaAs QWs. These indirect excitons have a lifetime of ~300 ns (for perpendicular electric fields of ~10^6 V/m),[12] while the lifetimes of direct excitons are in the order of 1 ns.[13] The excitonic drift of such indirect, long-living excitons is induced by applying a voltage drop V_Δ across a resistive top gate [Fig. 1(a)]. Mediated by the QCSE, the laterally varying electric field beneath the gate strip creates an in-plane excitonic potential gradient ∇U_{exc}. Due to the force $F = -\nabla U_{\mathrm{exc}}$, the excitons drift along the gradient towards regions of high electric fields [Fig. 1(b)].[7,11] Our TOF setup allows directly measuring the drift velocity v_d as a function of the applied gradient ∇U_{exc}. Defining the excitonic mobility as μ_{exc}

$= v_d / \nabla U_{\mathrm{exc}}$, we find experimental values of μ_{exc} exceeding 10^5 cm^2/eV s and corresponding exciton scattering times larger than 15 ps at 3.7 K. Both values exceed previous results on coupled QWs by a factor of 200.[11] At the same time, the scattering times compare reasonably well with electron scattering times in GaAs QWs. For temperatures higher than 10 K the excitonic drift is limited by phonon-scattering processes.

The starting point is an epitaxially grown AlGaAs/GaAs heterostructure containing two GaAs QWs encompassed by AlGaAs barriers [Fig. 1(a)]. Each QW has a thickness of 8 nm, while the QWs are separated by a 4-nm-thick tunnel barrier made out of Al$_{0.3}$Ga$_{0.7}$As. The QWs are located 60 nm below the surface of the heterostructure. A *n*-doped GaAs layer at a depth of $d = 370$ nm serves as back gate, and a semitransparent titanium layer is used as the top gate of the field effect structure. The metal gates, prepared by standard
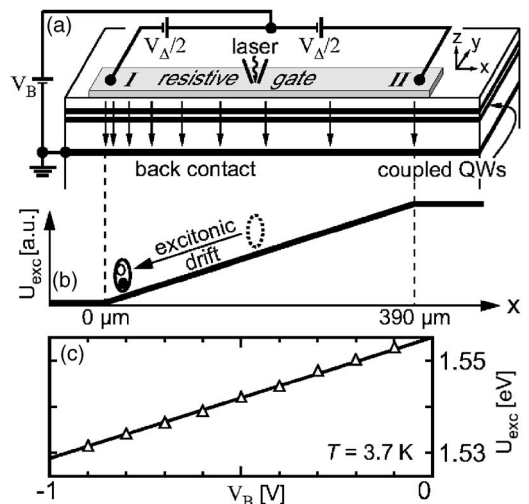

FIG. 1. (a) Excitonic time-of-flight apparatus. A current-carrying top gate (gray) defines a laterally varying vertical electric field (vertical arrows). (b) Sketch of the in-plane excitonic potential between contacts "I" and "II" due to the quantum confined Stark effect (QCSE). The slope of the gradient is tunable via the voltage V_Δ. (c) Calibration of the QCSE shift by application of a dc voltage V_B to the top gate.

[a)]Author to whom correspondence should be addressed; electronic mail: alex.holleitner@physik.uni-muenchen.de

optical lithography, typically have a thickness of 10 nm, a width of 50 μm, and a length ranging between 500 and 1000 μm. The resistance of such a gate strip is between 2 and 4 kΩ depending on its length.

The excitonic drift experiments are carried out in a helium continuous-flow cryostat in combination with a micro-photoluminescence setup in the temperature range between 3.5 and 40 K. The excitons are locally excited by focusing a pulsed laser onto the center of the top gate. The laser is operated at a pulse length of 50 ns and at a repetition period of 10 μs. At a spot diameter of ~10 μm the power density is 5 kW/cm^2. The laser wavelength is chosen to be 680 nm, such that electron-hole pairs are only created in the GaAs QWs and not in the AlGaAs barriers. For the TOF experiments, the PL signal of the recombining excitons is picked up by the optical microscope as a function of the delay time with respect to the initial laser pulse. The optical signal is subsequently guided through a triple-grating imaging spectrometer. An attached fast-gated, intensified charge coupled device (CCD) camera with an exposure time of 5 ns detects the PL emission of the excitonic cloud as a function of energy and space. In order to yield a sufficient signal to noise ratio, all images shown are taken by integrating over 2 $\times 10^7$ single events.

In Fig. 1(c) we calibrate the shift of the exciton energy due to the QCSE as a function of the applied voltage V_B at $V_\Delta = 0$ V. The energy U_{exc} of the spatially indirect excitons is shifted to lower values by $\Delta U_{exc} = edE_z$, with d the center distance of the two QWs and E_z the electric field perpendicular to the QWs. The data in Fig. 1(c) nicely follow a linear dependence with a slope of $\partial U_{exc}/\partial V = 26.4$ meV/V. The redshift is independent of the bath temperature T up to 30 K. For the TOF experiments, a constant bias voltage V_B of -0.4 V is applied to the top gate with respect to the grounded back contact at all times. 50 ns after the laser has been switched off, all short-living direct excitons have decayed and only indirect excitons remain. Due to diffusion such a cloud of mobile indirect excitons has typically a full width at half maximum diameter of about 80 μm, in accordance with previous results.[14,15]

We define $t=0$ as the point of time when the voltage drop V_Δ is applied across the resistive gate strip. In turn, the voltage between contacts "I" and "II" increases linearly along the gate strip. This voltage configuration creates a QCSE-mediated excitonic gradient potential ∇U_{exc} as sketched in Fig. 1(b). In turn, the excitons are exposed to a force $F = -\nabla U_{exc} = ed\nabla |E_z|$.[12] Since V_Δ is widely tunable, the method allows studying the in-plane drift of indirect excitons at different velocities. Figure 2 shows three subsequent CCD snapshots with 5 ns exposure time for $V_\Delta = 2$ V at (a) $t=0$, (b) $t=20$ ns, and (c) $t=40$ ns. Each image exhibits the lateral distribution of the excitons resolved in space (vertical axis) and in energy (horizontal axis). The distributions are tilted off the horizontal orientation in all snapshots, proving that the gate strip creates an in-plane gradient of the excitonic energy. Under the given experimental conditions, the linear gradient $\nabla U_{exc} \sim 100$ μeV/μm obtained from the tilt in Figs. 2(b) and 2(c) agrees well with the value for the dc-QCSE energy shift presented in Fig. 1(c). The lower energy gradient in Fig. 2(a) is due to an RC constant of the resistive gate of <10 ns which governs the rising behavior of V_Δ.

In Fig. 2(b) [Fig. 2(c)] the center of the excitonic cloud has traveled (23.3 ± 1.1) μm $[(47.4 \pm 1.8)$ μm$]$ away from the

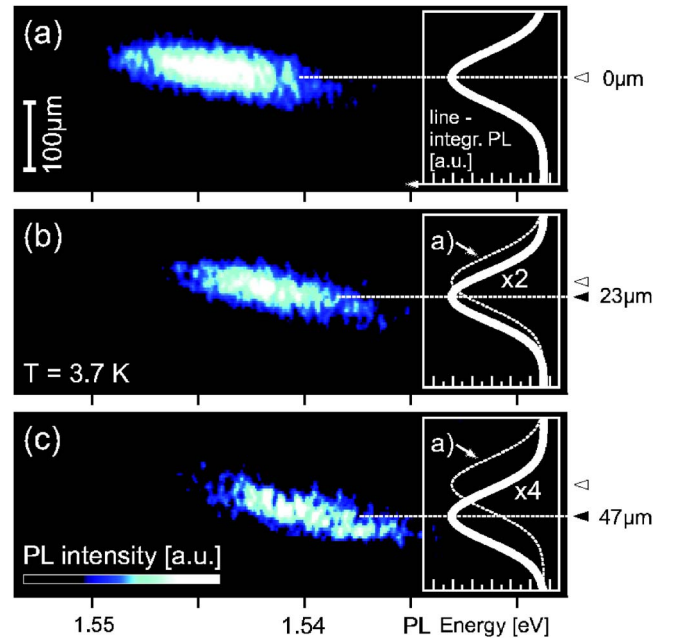FIG. 2. (Color online) Photoluminescence images showing drift of excitons at $T=3.7$ K, taken at (a) $t=0$ ns, (b) $t=20$ ns, and (c) $t=40$ ns after enabling the excitonic gradient potential. Insets: Energy-integrated representations of the data (solid curves). In the insets of (b) and (c) the lateral PL distribution of the cloud at $t=0$ ns is shown as a dashed curve.

excitation spot towards electrode I as defined in Fig. 1(a). At the same time, the excitons have reduced their energy by ~2 meV [~4 meV]. As a function of the delay time, the center of the excitonic distribution follows a diagonal path with respect to space and energy within the error bars (data not shown). The corresponding gradient $\partial U_{exc}/\partial V \sim 25$ meV/V again agrees well with the gradient obtained from the dc measurements in Fig. 1(c). This experimental finding proves that we study the drift dynamics specifically of indirect excitons. In addition, we would like to note that due to the finite lifetime of the indirect excitons the PL intensity in Figs. 2(b) and 2(c) has decreased by factors of 2 and 4, respectively.

By following the temporal evolution of the center of the cloud in Fig. 2, the excitonic drift velocity v_d can be directly determined. Figure 3(a) shows the dependence of v_d on the voltage drop V_Δ for various bath temperatures. At low temperatures we observe a maximum velocity of about ~2.5 $\times 10^3$ m/s. Experimentally, a leakage current I_L between the top and the back gate limits further increase of V_Δ and thus v_d. For $V_\Delta \leqslant 2.5$ V we find I_L to be $\leqslant 1$ μA. In this regime, a linear fit of the data gives the differential mobility μ_{exc} of the excitons defined as

$$\mu_{exc} = L(dv_d/dV_\Delta)(-\partial U_{exc}/\partial V)^{-1}. \tag{1}$$

Figure 3(b) summarizes the differential mobility μ_{exc} of indirect excitons at various temperatures. At low temperature, a constant mobility μ_{const} larger than 10^5 cm^2/eV s is observed, which exceeds previous results by a factor >200.[11] Recent publications on GaAs QWs suggest that the maximum mobility in our experiment is only limited by barrier alloy scattering,[16] which is independent of temperature (dashed dotted line). With increasing temperature the excitonic mobility decreases as $\mu_{po} \propto T^{-6}$ (dotted line), which is usually referred to enhanced scattering of excitons by polar optical phonons.[17] The combination of both scattering pro-
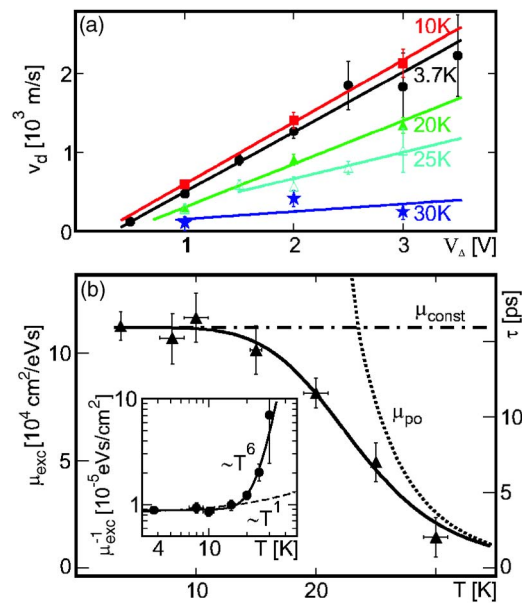
FIG. 3. (Color online) (a) Measured excitonic drift velocity v_d vs the voltage drop V_Δ at various bath temperatures T. The differential mobility is obtained from linear curves fitted to the data. (b) Excitonic mobility μ_{exc} and scattering time τ (right vertical axis) as a function of the temperature. Inset: Double logarithmic representation of the inverse mobility $1/\mu_{exc}$ vs temperature. The solid lines are theoretical fits to the data.

electron mobility is proportional to the sixth power of the QW width,[18] future experiments will aim towards wider QWs.

In summary, we explore the quantum confined Stark effect in combination with a resistive top gate to study drift dynamics of indirect excitons in coupled GaAs quantum wells. The emitted photoluminescence of the drifting excitons is resolved in space, energy, and time, which allows measuring the drift velocity and mobility of the excitons. At low temperatures we observe a maximum mobility of 10^5 cm^2/eV s which is a factor of 200 times larger than previous results on long-living excitons in coupled quantum wells.

cesses according to Matthiessen's rule explains the experimental data well (solid line). We would like to note that polar optical phonon scattering is usually expected for temperatures above 100 K.[17] However, as seen in the inset of Fig. 3(b), acoustic phonon scattering ($\propto T^{-1}$) cannot explain the data (dashed line).[16] In addition, we can calculate the transport scattering time $\tau \equiv \mu_{exc} m^*_{exc}$, with $m^*_{exc} = (m^*_e + m^*_h) \approx 0.25 m_e$ the effective exciton mass, $m^*_{e,h}$ the effective electron/hole masses in GaAs, and m_e the free electron mass [right axis in Fig. 3(b)]. Assuming the Einstein relation $D_{exc} = \mu_{exc} k_B T$, we can furthermore estimate an excitonic diffusion constant D_{exc} which corresponds to the measured drift mobility. At a temperature of 3.7 K we find an excitonic diffusion constant D_{exc} of about 30 cm^2/s. The latter is a factor of 100 larger than values obtained in the purely diffusive regime.[14] Since the PL signal depends on the temperature as well, TOF experiments above 30 K are ambiguous. Generally, the data shown are obtained from different samples patterned on one AlGaAs/GaAs wafer. Since the

[1] L. V. Keldysh and A. N. Kozlov, Sov. Phys. JETP **27**, 521 (1968).

[2] D. P. Trauernicht, A. Mysyrowicz, and J. P. Wolfe, Phys. Rev. B **28**, 3590 (1983).

[3] K. Kash, J. M. Worlock, M. D. Sturge, P. Grabbe, J. P. Harbison, A. Scherer, and P. S. D. Lin, Appl. Phys. Lett. **53**, 782 (1988).

[4] V. Negotia, D. W. Snoke, and K. Eberl, Appl. Phys. Lett. **75**, 2059 (1999).

[5] P. C. M. Christianen, F. Piazza, J. G. S. Lok, J. C. Maan, and W. van der Vleuten, Physica B **249**, 624 (1998).

[6] L. V. Butov, C. W. Lai, A. L. Ivanov, A. C. Gossard, and D. S. Chemla, Nature (London) **417**, 47 (2002).

[7] S. Zimmermann, A. O. Govorov, W. Hansen, J. P. Kotthaus, M. Bichler, and W. Wegscheider, Phys. Rev. B **56**, 13414 (1997).

[8] T. Huber, A. Zrenner, W. Wegscheider, and M. Bichler, Phys. Status Solidi A **166**, R5 (1998).

[9] J. Krauß, A. Wixforth, A. V. Kalameitsev, A. O. Govorov, W. Wegscheider, and J. P. Kotthaus, Phys. Rev. Lett. **88**, 036803 (2002).

[10] A. T. Hammack, N. A. Gippius, Sen Yang, G. O. Andreev, L. V. Butov, M. Hanson, and A. C. Gossard, J. Appl. Phys. **99**, 066104 (2006).

[11] M. Hagn, A. Zrenner, G. Böhm, and G. Weimann, Appl. Phys. Lett. **67**, 232 (1995).

[12] A. Gýrtner, D. Schuh, and J. P. Kotthaus, Physica E (Amsterdam) **32**, 195 (2006).

[13] J. Feldmann, G. Peter, E. O. Göbel, P. Dawson, K. Moore, C. Foxon, and R. J. Elliott, Phys. Rev. Lett. **59**, 2337 (1987).

[14] Z. Vörös, R. Balili, D. W. Snoke, L. Pfeiffer, and K. West, Phys. Rev. Lett. **94**, 226401 (2005).

[15] L. S. Levitov, B. D. Simons, and L. V. Butov, Phys. Rev. Lett. **94**, 176404 (2005).

[16] H. Hillmer, A. Forchel, S. Hansmann, M. Morohashi, E. Lopez, H. P. Meier, and K. Ploog, Phys. Rev. B **39**, 10901 (1989), and references therein.

[17] P. K. Basu and P. Ray, Phys. Rev. B **44**, 1844 (1991).

[18] H. Sasaki, T. Noda, K. Hirakawa, M. Tanaka, and T. Matsusue, Appl. Phys. Lett. **51**, 1934 (1987).